

## CHAPTER FIFTY FIVE

### Numerical Simulations of the 1964 Alaskan Tsunami

James R. Houston<sup>1</sup> and H. Lee Butler<sup>2</sup>, A.M. ASCE

#### Introduction

Tsunamis are long-period water waves usually generated by earthquakes. They occur predominantly in the Pacific Ocean and can produce massive inundation and destruction. The last major tsunami that seriously impacted the United States was the 1964 Alaskan tsunami. This tsunami was generated in Alaska and caused damage in Alaska, the Hawaiian Islands, and on the west coast of the continental United States. It is the most documented of all tsunamis and the only tsunami for which there is information on the ground motion that generated the tsunami.

Numerical models have been used to simulate tsunami generation and propagation. A numerical simulation of the 1964 Alaskan tsunami that included deep ocean propagation was performed by Hwang et al. (1) and a comparison was made with a deep water gage at Wake Island. Houston (2) performed a numerical simulation of this tsunami including both deep ocean and nearshore propagation in the Hawaiian Islands and presented comparisons with tide gage recordings. Although Houston (2) demonstrated the ability of numerical models to propagate tsunamis from source regions to distant shorelines, the Hawaiian Islands considered in his simulation have a very short continental shelf and the conclusions of his study might not be applicable to typical continental areas that have significantly longer continental shelves.

There has been considerable controversy in recent years concerning the governing equations for tsunami generation, deep ocean propagation, propagation over the continental shelf, and land inundation. The importance of frequency dispersion and nonlinearity in tsunami propagation has been debated. However, research by a number of investigators in recent years has provided clear evidence of the relative significance of frequency dispersion and nonlinearities. The numerical simulation presented in this paper of the 1964 Alaskan tsunami and comparisons with tide gage recordings of this tsunami all along the west coast of the continental United States provide additional confirmation of the conclusions of these investigators. I show that for very large tsunamis such as the 1964 Alaskan tsunami, frequency dispersion is negligible during

<sup>1</sup>Chief, Research Division, Coastal Engineering Research Center, U. S. Army Engineer Waterways Experiment Station, P. O. Box 631, Vicksburg, MS 39180-0631.

<sup>2</sup>Chief, Coastal Processes Branch, Coastal Engineering Research Center, U. S. Army Engineer Waterways Experiment Station, P. O. Box 631, Vicksburg, MS 39180-0631

all phases of tsunami propagation except in rare circumstances when tsunamis exhibit a bore-like form in their final runup phase. Nonlinearities also are negligible except during tsunami land inundation, and they are not generally dominating even during inundation by non-bore waves.

It should be emphasized that the conclusions of this paper are valid only for spatially large tsunamis such as the 1964 Alaskan tsunami and for the first major waves recorded at distant locations. Frequency dispersion may be significant for the propagation of relatively short period tsunamis generated by ground displacements that are small and for the later waves of even large tsunamis. Waves near the tsunami source region may be influenced by details in the time-history of the ground motion or by small scale features of the permanent ground deformation.

#### Governing Equations

Tuck (3) made the following sweeping statement in a paper on models of tsunami propagation: "The linear long-wave equations are adequate to describe most of the tsunami generation, propagation and reception processes."

He primarily used intuitive arguments based upon the magnitudes of ratios of tsunami wave lengths and wave heights to water depths. Tuck (3) clearly stated that his conclusions applied only to large tsunamis such as the 1964 Alaskan tsunami, but the considerable disagreements with his conclusions that developed were a result of assumptions that his statement applied to smaller tsunamis.

Hammack (4) in a series of detailed laboratory experiments and calculations employing the Korteweg and deVries (KdV) equation (includes frequency dispersive and nonlinear terms) concluded that linear theory is applicable for determining tsunami generation for large tsunamis such as the 1964 Alaskan tsunami. In subsequent work using the KdV equation, Hammack (5) concluded ". . . the propagation of the lead wave of a two-dimensional tsunami is modeled by linear nondispersive theory for almost its entire trajectory. The KdV equation is valid, but unnecessary, while linear dispersive theory never applies." This trajectory was explained to extend from the source region to the vicinity of a beach. Nonlinearities were found to be negligible in the generation region and for deep ocean propagation. Frequency dispersion was shown to be negligible for the lead wave of the 1964 Alaskan tsunami until it propagated a length of time of approximately 100 hours (equivalent to a propagation distance of approximately 50,000 miles). Kajiura (6) in a separate analysis using linear but dispersive equations found "The remarkable similarity of results between dispersive and nondispersive theories is evident for  $P_a = 4$ ."  $P_a$  was defined as

$$P_a = 6(h/g)^2/t^3(b/h) \quad (1)$$

where

h = water depth

g = acceleration of gravity

t = time  
b = one-half the length of the major axis of an elliptical source region

Using parameters for the 1964 Alaskan tsunami,  $P_a$  decreases to a value of 4 after 105 hours. Thus Kajiura's analysis is in agreement with that of Hammack (4). Kajiura (6) also noted the calculations of Carrier (7) were in similar agreement.

The unimportance of nonlinearities and frequency dispersion for generation and deep ocean propagation of large tsunamis was confirmed by simulations of the 1964 Alaskan tsunami and comparisons of results with a deep water gage at Wake Island (1) and with tide gages in the Hawaiian Islands (2). These simulations did not confirm the negligibility of nonlinearities during propagation from the deep ocean to shore, since the Wake Island gage is in deep water and the continental shelf of the Hawaiian Islands is so short that the time scale for the growth of nonlinearities is small.

Hammack (5) considered tsunami propagation from the deep ocean to the nearshore area using the KdV equation and concluded that ". . . linear nondispersive theory can be used until the distance across the continental shelf (of uniform depth) that the lead wave propagates is given by . . . X = 200 miles." Goring (8) conducted laboratory experiments and calculations using Boussinesq equations (similar to the KdV equations, but allowing wave propagation in two directions) and also concluded ". . . the propagation of tsunamis from the deep ocean to the continental shelf-break and for some distance onto the shelf will be predicted as well by the linear nondispersive theory as by the nonlinear theories." The conclusions of Hammack (5) and Goring (8) may not be in agreement with calculations of Mader (9) who used a Simplified Marker and Cell (SMAC) code that included vertical accelerations and nonlinearities and a vertically integrated linear long wave code (SWAN). Significant differences were noted between the calculations of the SMAC and SWAN codes for long waves propagating over a simulated continental shelf (9). However, since experimental or field data are not presented, differences between the models noted by Mader (9) are likely attributable to inaccuracies of the solution techniques, methods of application, or boundary conditions rather than to differences in the equations solved.

Tsunamis are often portrayed as bore-like walls of water during their final stages as they inundate coastal areas. However, tsunamis only rarely appear as bore-like along coastlines distant from a source region. Instead they normally are described as having the appearance of "fast-rising" tides. In this form they are likely to be governed by nonlinear long wave equations that are successfully used for tidal inundation problems.

#### Simulation of the 1964 Alaska Tsunami

Tsunami generation and deep ocean propagation was simulated using a finite-difference numerical model (1). The model solves the linear long-wave equations on a spherical coordinate grid. One-third by one-third degree grid cells were used with the grid extending over much of the

north Pacific Ocean. The boundary condition employed on land boundaries of the grid was the component of the velocity normal to the boundary was equal to zero. On open (ocean) boundaries, a first-order approximation of total transmission was made.

The model solved an initial value problem starting with an uplift deformation of the water surface identical with the major features of the permanent deformation (permanent in the sense that the time scale associated with it is much longer than the period of the tsunami) of the seafloor following the 1964 earthquake. The transient movements within the time history of the ground motion of the 1964 earthquake were neglected because Hammack (4) has shown through laboratory experiments that these movements are unimportant in the far field for spatially large ground motions. Hammack (4) has further shown that the initial deformation of the water surface will closely approximate major features of the permanent deformation of the ocean floor, provided these features have characteristic lengths that are at least four times as great as the water depth (water depth was approximately 200 m in the tsunami source region of the 1964 earthquake). The neglect of smaller features is unimportant because Hammack (4) demonstrated in laboratory experiments such small-scale details produce waves negligible in the far field. These experiments (4) have great practical significance, since details of the time history of ground motion and small scale features of the ground deformation are unknown for the 1964 earthquake and other tsunamigenic earthquakes.

The permanent deformation of the ocean's bottom as a function of spatial location for the 1964 earthquake was adapted (1) from the field measurements of Plafker (10). It is identical to the uplift used earlier by others (1,2). Starting with this uplift as an initial condition, the numerical model propagated the 1964 tsunami across the deep ocean to the west coast of the continental United States.

The cell size of the deep ocean grid is too coarse to allow accurate simulations of tsunami propagation from the deep ocean to shore, since the tsunami wave length decreases in shallow water. Therefore, separate finite difference grids were used to propagate waves from a water depth of 500 m to shore. a variable rectilinear grid was used with grid cells that decreased in size as the water depth decreased. The smallest grid cells were less than 1 mi on a side. A finite-difference numerical model (11) was used to calculate nearshore propagation. The model uses a highly efficient implicit solution scheme that employs a centered, alternating-direction procedure. Nonlinear long wave equations including bottom function terms were solved. However, in agreement with the calculations of Hammack (5) and Goring (7) it was found that the results were insensitive to the nonlinear advective and bottom friction terms for reasonable values of bottom friction.

Figures 1-9 show comparisons between the numerical model calculations and tide gage recordings for nine tide gates on the west coast of the continental United States. These are all of the tide gages on the west coast that recorded the 1964 tsunami, except for gages in Puget Sound, the Columbia River, and San Francisco Bay (not covered by numerical grid). The tide has been extracted from all the comparisons except

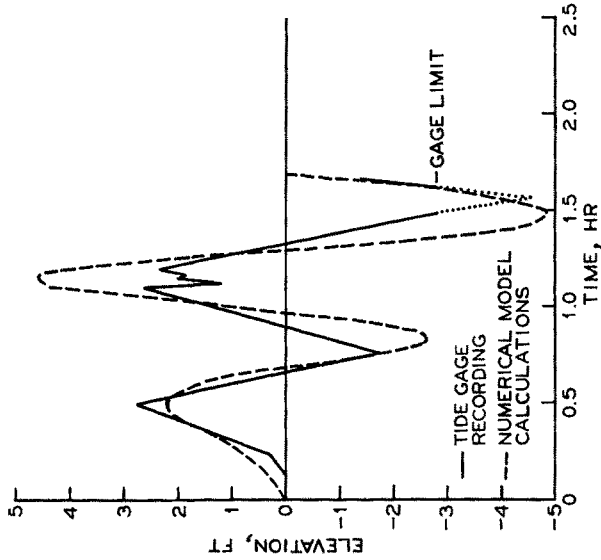


Figure 1. 1964 Tsunami at Rincon Island, California.

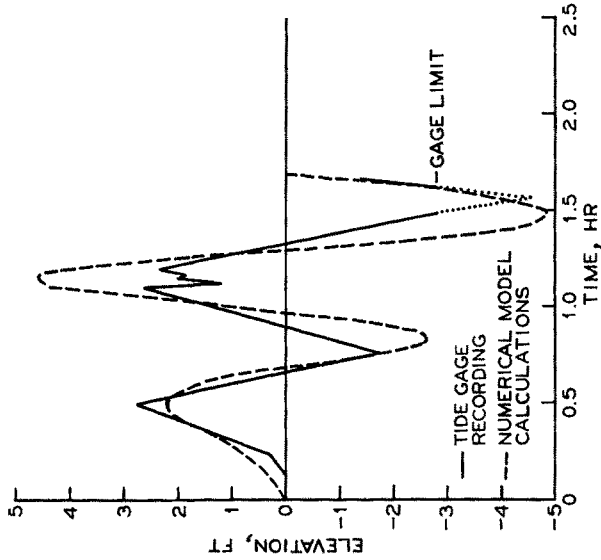


Figure 2. 1964 Tsunami at Santa Monica, California.

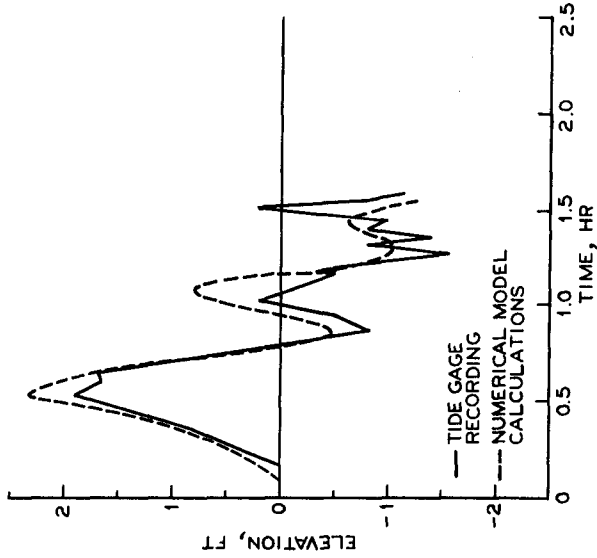


Figure 4. 1964 Tsunami at Alamites Bay, California.

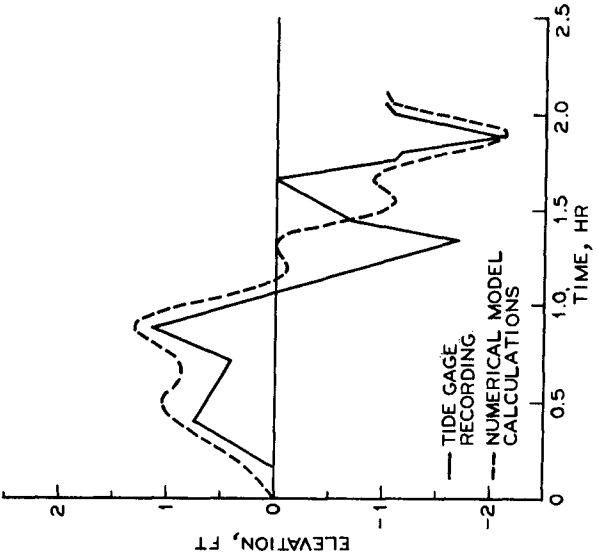


Figure 3. 1964 Tsunami at Los Angeles (Berth 60), California.

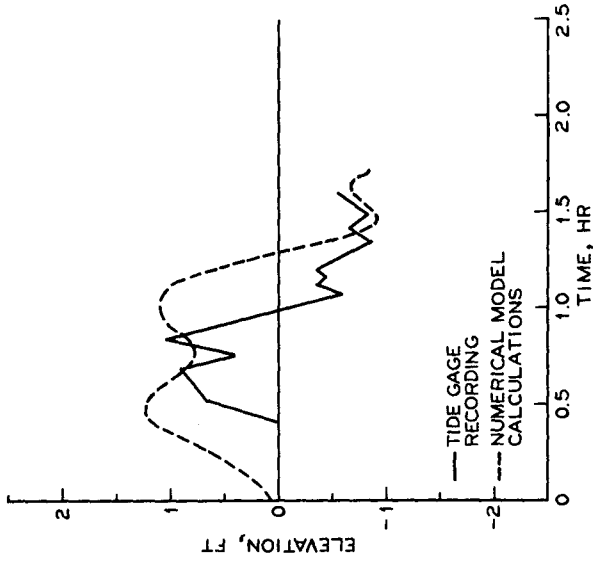


Figure 6. 1964 Tsunami at San Diego, California.

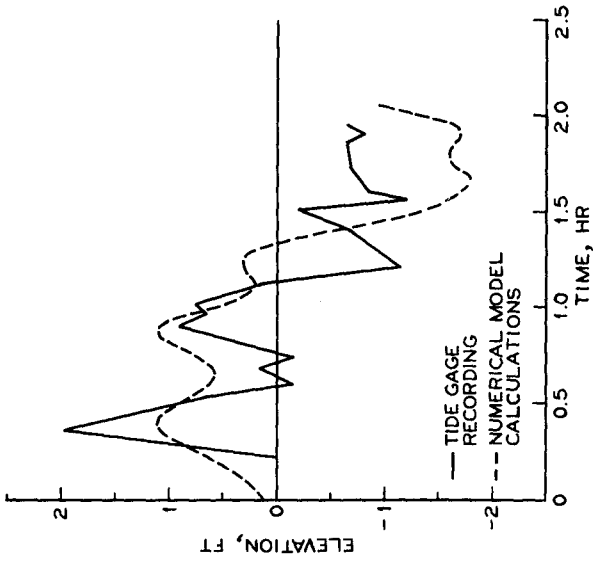


Figure 5. 1964 Tsunami at La Jolla, California.

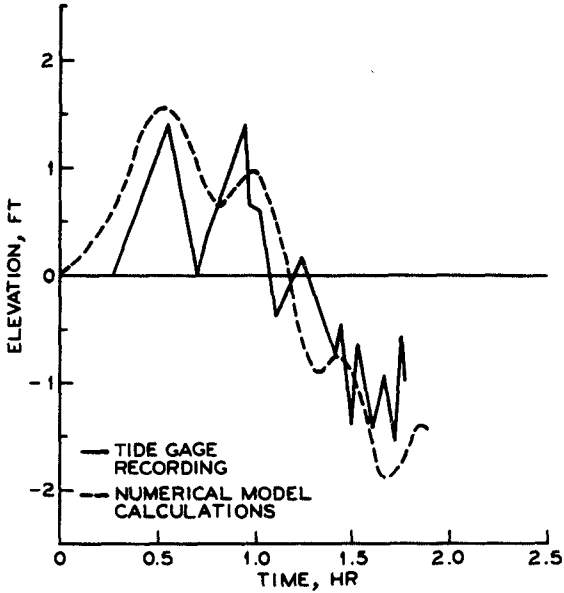


Figure 7. 1964 Tsunami at Newport Bay, California

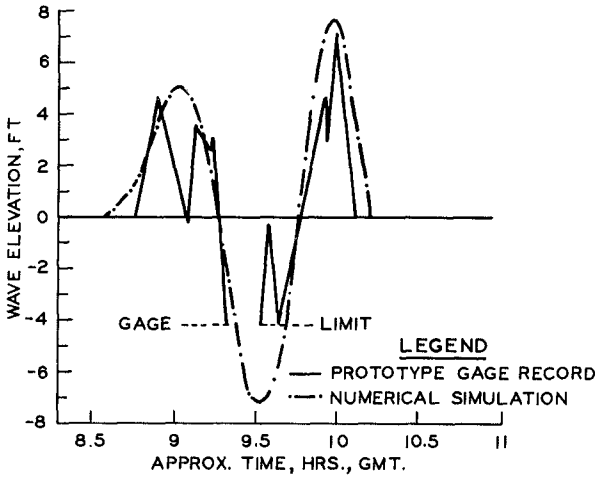


Figure 8. 1964 Tsunami at Avila Beach, California.

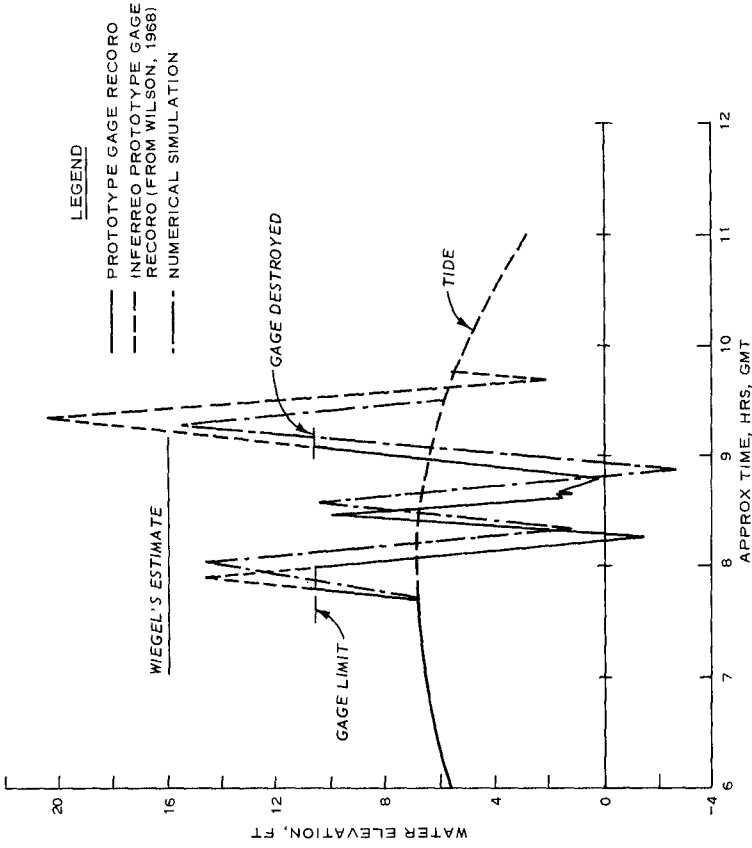


Figure 9. 1964 Tsunami at Crescent City, California.

the one at Crescent City, California. A tide gage record of the 1964 tsunami at Crescent City inferred by Wilson and Torum (12) is used for the comparison at Crescent City. In addition, an estimate by Wiegel (13) that differs somewhat from the estimate of Wilson and Torum (12) is presented. Each comparison is over a period of 1.5 to 2.0 hr.

Tide gages do not record tsunamis perfectly, but the heights and periods of the waves seen in Figures 1-9 are such that gage response is close to 100 percent (14). However, the standard sampling interval of tide gages is 6 minutes and this long sampling interval distorts the recorded wave form and can reduce apparent heights. Tide gages also experienced difficulties when gage limits were encountered. In addition to truncations of the waveforms as seen in Figures 2, 8, and 9, gage limit problems are seen in the inverted trough of Figure 8 and high frequency oscillations in the crests seen in Figures 2 and 8.

The wave form recorded at one location is remarkably different from those recorded at other locations. The waveforms for the 1964 tsunami calculated for the Hawaiian Islands (2) also show remarkable differences from gage to gage. The numerical calculations are in good general agreement with the waveforms. The shape of the waveforms, and wave heights and periods are in reasonable agreement in Figures 1-9 considering unknowns of the source region. Calculated maximum wave heights vary among the locations from as little as 1.5 ft to as much as 18.0 ft.

#### Land Inundation

The only gage location where the tsunami produced significant land inundation was at Crescent City, California. Figure 10 shows the numerical grid used to simulate land inundation at Crescent City. The grid was oriented such that the incident waves approached Crescent City from the direction predicted by Roberts and Kauper (15). The interaction of the tsunami with the Crescent City region was quite complex. For example, the Crescent City Harbor is protected by breakwaters, some of which were overtopped and others which were not. In the region there is a developed city area, mud flats, and an extensive riverine floodplain. Inland flooding was extensive in the floodplain area and extended as much as a mile inland. Sand dunes and elevated roads played a prominent role in limiting flooding in certain areas.

The input to the numerical model was a wave crest that, when propagated to shore, reproduced as accurately as possible the historical maximum elevation at the tide-gage location near the shoreline in Crescent City. There is some disagreement among investigators on the maximum elevation of the tsunami at the tide gage with estimates ranging from 18 to 20.7 ft above mean lower low water (mllw). A wave crest with an elevation of 19 ft above mllw at the tide-gage location was used in this simulation, based on a study by Keulegan et al. (16) that considered all available data and concluded the 19.0-ft level was the most likely.

There are several barriers in the Crescent City region. Wiegel (13) reports that there was little flow over the outer breakwater during the 1964 tsunami (Figure 10). Therefore, this breakwater was represented as a non-overtopping barrier. However, the breakwaters attached to Whaler

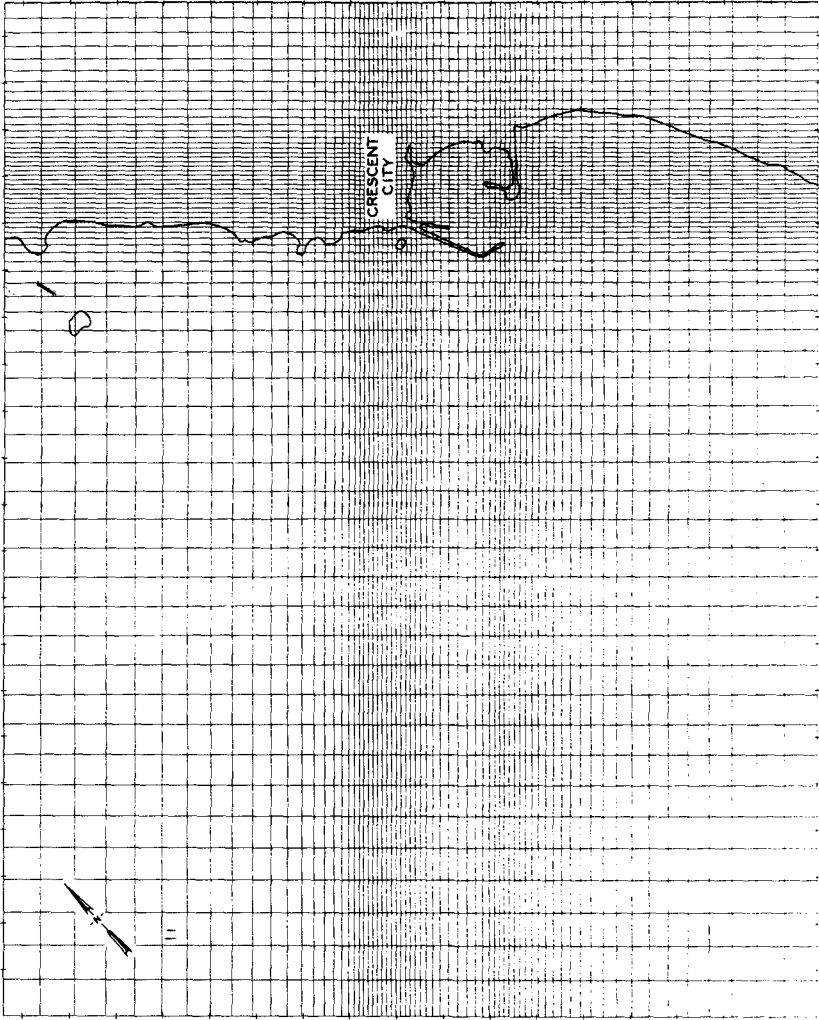


Figure 10. Numerical grid from Crescent City, California.

Island (Figure 11) were overtopped during a part of the tsunami and thus are represented as dynamic overtopping barriers. Similarly, Redwood Highway (Figure 11); and beach dunes along the crest were overtopped during the tsunami. Magoon (17) reported water flowed over these barriers with flow rates governed by weir equations.

Frictional effects in the numerical model are governed by Chezy frictional coefficients. Values of Manning's  $n$  suggested by Bretschneider and Wybro (18) for coastal terrain were used. Manning's  $n$  values were selected for very general categories of terrain, since detailed knowledge of vegetation and land roughness are not known. The ocean bottom, mud flats, and beaches were assigned a value of 0.024. Developed areas were assigned a value of 0.035 and the riverine flood-plain area and other heavily vegetated areas a value of 0.055. No attempt was made to force agreement of numerical calculations and historical recordings of elevations by varying local values of Manning's  $n$ .

The U. S. Army Corps of Engineers made surveys of the tsunami inundation at Crescent City in January, April, and May of 1965 (17). Figure 11 shows the location of 11 high-water marks recorded by the surveys. The tide gage was located near high-water mark No. 307 (Figure 11). Table 1 presents the measured elevations at the high-water marks and elevations calculated by the numerical model. The measured and calculated elevations are within 1 ft except at locations 307, 2, 3, and 5. However, Wiegel (13) reports that the measured elevation at

Table 1

High-Water Mark Number (Reference 17)	Measured Elevation mllw, ft	Calculated Elevation mllw, ft	Difference ft
302	18.35	17.95	+0.40
305	18.74	19.39	-0.65
307	20.70	19.45	+1.25
309	19.84	19.79	+0.05
312	19.41	20.23	-0.82
316	16.29	17.09	-0.80
1	15.90	15.43	+0.47
2	17.80	19.24	-1.44
3	19.30	18.89	+0.41
4	16.50	18.94	-2.44
5	20.50	19.13	1.37

location 307 was greater than the actual wave elevation by 1 to 2 ft due to local runup on a concrete wall. Thus the actual wave elevation and the calculated elevation are in good agreement at location 307. The measured elevation at location 4 is lower than the calculated elevation, since the measured high-water mark was inside a lumber building (17). Incomplete filling of the lumber building by water would result in lower elevations within the building than outside the building. Location 5 is almost 2 miles south of the tide gage. It is likely the wave approaching this shoreline had a greater elevation than the wave approaching the harbor area. The elevation calculated at this location could be increased by varying the incident wave form along the input boundary.

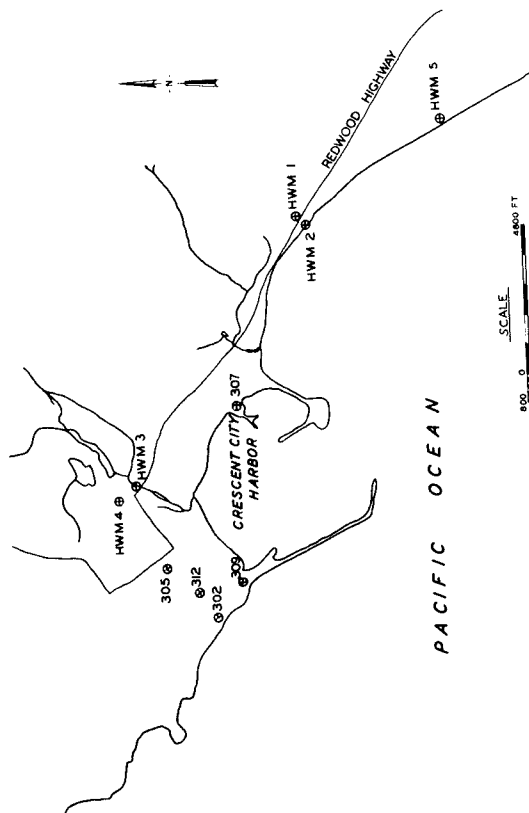


Figure 11. High-water mark locations for 1964 Tsunami (adapted from Magoon, 1965).

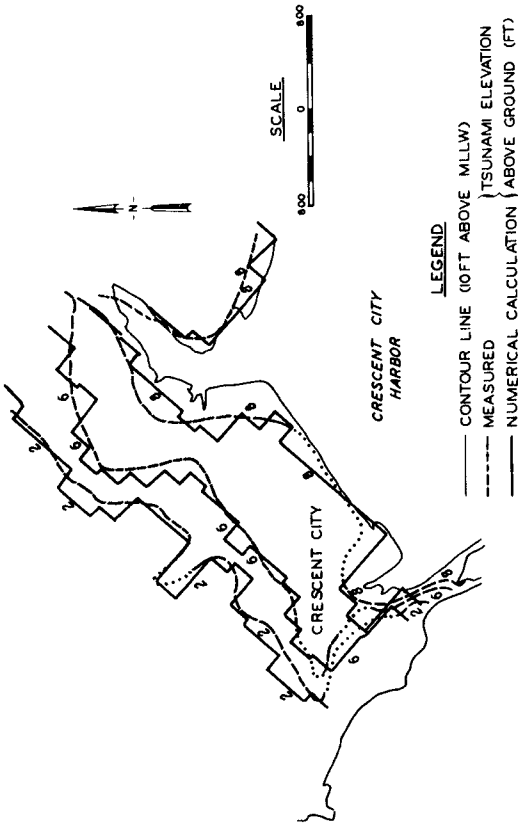


Figure 12. Inundation Lines, 1964 Tsunami (adapted from Magoon, 1965).

There is no apparent explanation for the disagreement at location 2, especially since there is good agreement at nearby location 1.

The agreement between the measured high-water marks and calculated elevations is quite good. The root-mean-square error is 0.7 ft (elevations at locations 307, 4, and 5 not included since differences attributable to factors other than the numerical model). Since the observed elevation at the tide gage used to choose an incident wave height is accurate to within no more than 0.5 to 1.0 ft, the agreement between measured and calculated elevations is good.

Figure 12 shows contour lines of the tsunami elevation above ground level within the developed area of Crescent City. The topography and tsunami elevations are known in much more detail in this developed area than any other area. The dotted parts of the measured elevation denote uncertain elevations. The contour lines for the calculated elevations were determined by linear interpolation. For example, if the elevation at the center of one cell was 9.0 ft above land and the elevation in an adjacent cell was 7.0 ft, the contour line was drawn halfway between the two cell centers. The agreement between the measured and calculated elevations shown in Figure 12 is good.

#### Conclusions

Linear long waves are adequate to simulate tsunami generation, propagation across the deep ocean, and propagation over the continental shelf of the west coast of the continental United States or the Hawaiian Islands when the uplift that generates the tsunami is large spatially (1964 Alaskan or 1960 Chilean tsunamis). Tsunamis usually appear as rapidly rising water levels along distant coastlines. Nonlinear long wave equations that include bottom function terms (typically used to model astronomical tides) can be used to model land inundation for tsunamis that appear as rapidly rising water levels. If information exists on the ground motion that generates a tsunami, the tsunami can be simulated over its complete path of propagation from a generation region up to terminal flooding at a distant coastline.

#### Acknowledgments

The authors wish to acknowledge the Federal Emergency Management Agency for funding the studies on which this paper is based and the Office, Chief of Engineers, U. S. Army Corps of Engineers for authorizing publication of this paper.

#### Appendix.-References

1. Hwang, L. S., Butler, H. L., and Divoky, H. L., "Tsunami Model: Generation and Open-Sea Characteristics." *Bulletin of the Seismological Society of America*, Vol. 62, No. 6, 1972, pp. 1579-1596.
2. Houston, J. R., "Interaction of Tsunamis with the Hawaiian Islands Calculated by a Finite-Element Numerical Model," *Journal of Physical Oceanography*, Vol. 8, No. 1, 1978, pp. 93-101.
3. Tuck, E. O., "Models For Predicting Tsunami Propagation." *Proceedings of the National Science Foundation Tsunami Workshop*, Coto de Caza, California, 1979, pp. 43-104.

4. Hammack, J. L., "Tsunamis - A Model of Their Generation and Propagation," Report No. KH-R-28, California Institute of Technology, Pasadena, California, 1972.
5. Hammack, J. L., and Segur, H., "Modeling Criteria for Long Waves," Journal of Fluid Mechanics, Vol. 84, Pt. 2, 1978.
6. Kajiura, K., "Tsunami Generation," Proceedings of the National Science Foundation Tsunami Workshop, Coto de Caza, California, 1979, pp. 15-42.
7. Carrier, G. F., "The Dynamics of Tsunamis," Mathematical Problems in the Geophysical Sciences, Geophysical Fluid Dynamics, American Mathematical Society, 1, 1970, pp. 157-187.
8. Goring, D. G., "Tsunamis - The Propagation of Long Waves Onto a Shelf," Report No. KH-R-38, California Institute of Technology, Pasadena, California, 1978.
9. Mader, C. L., "Numerical Simulation of Tsunamis," Hawaii Institute of Geophysics, HIG-73, 3, 1973.
10. Plafker, G., "Tectonics of the March 27, 1964, Alaska Earthquake," U. S. Geological Survey Professional Paper 543-I, pp. 11-174, 1969.
11. Butler, H. L., "Numerical Simulation of Coos Bay-South Slough Complex," Technical Report H-78-22, U. S. Army Engineer Waterways Experiment Station, CE, Vicksburg, Mississippi, 1978.
12. Wilson, B. W., and Torum, A., "The Tsunami of the Alaskan Earthquake, 1964: Engineering Evaluation," Technical Memorandum No. 25, U. S. Army Coastal Engineering Research Center, CE, Washington, D. C., 1968.
13. Wiegel, R. L., "Protection of Crescent City, California, from Tsunami Waves," prepared for the Redevelopment Agency of the City of Crescent City, Berkeley, California, 1965.
14. Loomis, H. G., "The Nonlinear Response of a Tide Gage to a Tsunami," Proceedings of the 1983 Tsunami Symposium, Hamburg, Germany, 1983.
15. Roberts, J. A., and Kauper, E. K., "The Effects of Wind and Precipitation on the Modification of South Beach, Crescent City, California," ARG64 FR-186, Office of the Chief of Research and Development, Washington, D. C., 1964.
16. Keulegan, G. H., Harrison, J., and Mathews, M. J., "Theoretics in Design of the Proposed Crescent City Harbor Tsunami Model," Technical Report H-69-9, U. S. Army Engineer Waterways Experiment Station, CE, Vicksburg, Mississippi, 1969.
17. Magoon, O. T., "Structural Damage by Tsunamis," Coastal Engineering Santa Barbara Specialty Conference of the Waterways and Harbors Division, American Society of Civil Engineers, pp. 35-68, 1965.
18. Bretschneider, C. L., and Wybro, P. G., "Tsunami Inundation Prediction," Proceedings of the 15th Coastal Engineering Conference, American Society of Civil Engineers, pp. 1000-1024, 1975.